Surrogate Constructed Scalable Circuits ADAPT-VQE in the Schwinger model

Erik Gustafson[1,*] Kyle Sherbert[2,3,4,*] Adrien Florio[5] Karunya Shirali[3,4] Yanzhu Chen[3,4,6] Henry Lamm[7,8] Semeon Valgushev[9] Andreas Weichselbaum[5] Sophia E. Economou[3,4] Robert D. Pisarski[5] and Norm M. Tubman[10]

[1] *Universities Space Research Association, Research Institute for Advanced Computer Science (RIACS) at NASA Ames Research Center, Mountain View California*
[2] *Department of Chemistry, Virginia Tech, Blacksburg, VA 24061*
[3] *Department of Physics, Virginia Tech, Blacksburg, VA 24061*
[4] *Virginia Tech Center for Quantum Information Science and Engineering, Blacksburg, VA 24061*
[5] *Department of Physics, Brookhaven National Laboratory, Upton New York*
[6] *Department of Physics, Florida State University, Tallahassee, FL 32306*
[7] *Superconducting and Quantum Materials System Center (SQMS), Batavia, Illinois, 60510, USA*
[8] *Fermi National Accelerator Laboratory, Batavia, Illinois, 60510, USA*
[9] *Iowa State University, Ames Iowa*
[10] *NASA Ames Research Center, Moffet Field California*[†]

(Dated: August 26, 2024)

Inspired by recent advancements of simulating periodic systems on quantum computers, we develop a new approach, $(SC)^2$-ADAPT-VQE, to further advance the simulation of these systems. Our approach extends the scalable circuits ADAPT-VQE framework, which builds an ansatz from a pool of coordinate-invariant operators defined for arbitrarily large, though not arbitrarily small, volumes. Our method uses a classically tractable "Surrogate Constructed" method to remove irrelevant operators from the pool, reducing the minimum size for which the scalable circuits are defined. Bringing together the scalable circuits and the surrogate constructed approaches forms the core of the $(SC)^2$ methodology. Our approach allows for a wider set of classical computations, on small volumes, which can be used for a more robust extrapolation protocol. While developed in the context of lattice models, the surrogate construction portion is applicable to a wide variety of problems where information about the relative importance of operators in the pool is available. As an example, we use it to compute properties of the Schwinger model — quantum electrodynamics for a single, massive fermion in $1+1$ dimensions — and show that our method can be used to accurately extrapolate to the continuum limit.

I. INTRODUCTION

State preparation is a crucial component of many quantum algorithms, including phase estimation and time evolution, in all areas of physical simulation from chemistry, to materials science, to high energy and nuclear physics [1–12]. Significant work has been done on state preparation for materials and chemical systems [13–23], and more recently in nuclear and high energy physics [24–33]. Notably, the Variational Quantum Eigensolver (VQE) can prepare ground states using shallow depth circuits [14, 34–38], and in particular, the Adaptive Derivative-Assembled Problem Tailored VQE (ADAPT-VQE) [39, 40] shows great promise in finding ground states with compact circuits for a wide variety of problems. In this algorithm, the variational quantum circuit is iteratively built by exponentiating simple operators greedily selected from a user-defined pool, where the coefficient for each operator is treated as a variational parameter. The operators in the pool determine the expressivity of the ansatz, while the size of the pool determines the measurement overhead required for implementation.

Systems in materials science and nuclear physics often have discrete translational invariance (i.e. periodicity). These systems are typically very challenging, since very large volumes are required to obtain physically meaningful results. However, variational algorithms can incorporate translational invariance with a variety of strategies, compatible with ADAPT-VQE. For example, one could adopt a momentum basis, such that all operators implicitly satisfy translational invariance [41]. Alternatively, one could use a local real-space basis, and "tile" operators to build up an operator pool, such that local interactions relevant in small volumes are systematically integrated into larger volumes [42]. Finally, one can enforce translational invariance in the real-space representation. This is the approach taken by [28, 31], which introduced the "Scalable Circuits" ADAPT-VQE variant, or SC-ADAPT-VQE.

In SC-ADAPT-VQE, one first solves the ADAPT-VQE problem for small volumes which are classically simulable, to obtain both a sequence of (translationally-invariant) operators and the optimal coefficients for each operator. One then extrapolates the coefficients to the thermodynamic (large-volume) limit, to obtain a circuit that can be run, without any further optimization, on quantum hardware. Refs. [28, 31] applied SC-ADAPT-

* Erik Gustafson and Kyle Sherbert contributed equally.
† norman.m.tubman@nasa.gov

VQE to study the Schwinger model [43–45], a prototypical theory of gauge fields with matter, to demonstrate a procedure of scalable circuits. Their work considered systems of sizes up to 32 qubits as "small", and demonstrated circuit viability on QPUs for "large" systems with over 100 qubits.

While the results in Refs. [28, 31] are impressive, ADAPT-VQE will tend to select a different sequence of operators for each different volume. This is especially true for the later operators needed to obtain high-accuracy trial states, and this can result in ambiguities extrapolating to large volumes. Furthermore, it is not yet clear whether these methods can be used to explore the regime where the lattice spacing goes to zero, an essential step to ensure that a lattice theory can be used to study the corresponding field theory in the continuum limit. Therefore, two crucial questions remain:

1. How can the SC-ADAPT-VQE framework be modified to obtain less ambiguous extrapolations to the thermodynamic limit?

2. Can the SC-ADAPT-VQE framework be used to obtain accurate extrapolations to the continuum limit?

To address the first question, we introduce Surrogate-Constructed Scalable-Circuits ADAPT-VQE, or $(SC)^2$-ADAPT-VQE. This new variant modifies SC-ADAPT-VQE in two ways: First, while one adopts the same translationally-invariant operator pool as in Refs. [28, 31], one uses a large-volume classical surrogate such as matrix product states (used in this work), density matrix renormalization groups, or classical coupled cluster equations to pre-screen the most relevant operators, reducing the size of the pool. Second, one solves ADAPT-VQE *just once*, on the largest classically emulateable volume, and then optimizes the coefficients for the *same operator sequence* on each smaller volume.

To address the second question, we use our $(SC)^2$-ADAPT-VQE method to perform extrapolations to the infinite volume (thermodynamic) limit, for a series of systems with reduced lattice spacing. We then extrapolate the thermodynamic limit results for each problem instance to the continuum limit, where the lattice spacing vanishes. We demonstrate that, even in the absence of large-volume runs on quantum hardware, the $(SC)^2$-ADAPT-VQE ansatz provides a robust method to calculate observables in the continuum limit.

This paper is organized as follows. In Sec. II we discuss the target Hamiltonian for our studies, which is that of the Schwinger model, Refs. [28, 31]. We elaborate on VQE, ADAPT-VQE, and SC-ADAPT-VQE, in Sec. III. We describe our own method, $(SC)^2$-ADAPT-VQE, in Sec. IV. The results from our simulations, including extrapolations to the continuum limit for the massless Schwinger model, are provided in Sec. V. In Sec. VI we discuss the impact of this work, and future directions.

II. LATTICE FIELD THEORIES AND THE SCHWINGER MODEL

Before discussing our particular system, we offer a brief review of quantum computing for quantum field theories. The principal method for quantum simulations of field theories utilizes lattice models. In this method, the infinite dimensional Hilbert space is partially truncated by only utilizing a finite number of points in space, while leaving the remaining degrees of freedom unchanged; this leaves a finite number of locally infinite dimensional Hilbert spaces. A key requirement for quantum simulation is mapping the infinite dimensional Hilbert space to finite dimensional quantum resources. Significant work has been done to progress simulations of these models across a wide range of digitizations such as discrete groups [46–58], loop-string-hadron formulations [59–64], quantum link models [65–69], electric field truncations [28, 31, 70–87] and other novel formulations [88–96]. Additional work has been done on simulation methods for measuring observables [33, 97–101], road maps and resource estimates for simulations [73, 86, 102–105], proposals for simulations on hardware [84, 85, 87, 106–108], multigrid methods for quantum simulation[109], and state preparation techniques [25, 28, 31, 110–114]. Finally, there has also been complementary development of simulation tools and uses for quantum computation of field theories such as classical and classical-quantum feedback [115–122], error mitigation and correction schemes [123–131], more accurate Hamiltonians [132–134], improved circuits [135], reduced memory requirements [136, 137], uses for qudits [138–140], and other techniques and benchmarks [141, 142].

We use the lattice Schwinger model as a prototype field theory to showcase our $(SC)^2$-ADAPT-VQE algorithm, just as it was used by Refs. [28, 31] to showcase SC-ADAPT-VQE. The lattice Schwinger model is a spatial discretization of quantum electrodynamics in $1+1$ dimensions, with a single species of fermion. Due to its relative simplicity, this model from high energy physics has been studied extensively as a test case for quantum simulations [113, 143–152]. In fact it is closely related to a type of Heisenberg spin chain with alternating external magnetic fields. After integrating out the bosonic degrees of freedom and performing a Jordan-Wigner transformation, the Hamiltonian is

$$\begin{aligned}\hat{H} =& \frac{1}{2a}\sum_{j=0}^{N_s-2}(\hat{\sigma}_j^+\hat{\sigma}_{j+1}^- + \hat{\sigma}_{j+1}^+\hat{\sigma}_j^-) + \frac{m_0}{2}\sum_{j=0}^{N_s-1}(-1)^j\hat{\sigma}_j^z \\ &+ \frac{ag^2}{8}\sum_{j=0}^{N_s-2}(\sum_{k=0}^{j}(\hat{\sigma}_k^z + (-1)^k))^2, \end{aligned} \tag{1}$$

where m_0 is the bare mass of the fermion, g is the bare electric charge (coupling constant) for the gauge field [153], and N_s is the number of sites. With Kogut-Susskind (frequently referred to as staggered) fermions, N_s must be an even integer.

Note that in the rest of this work, we will consider the *massless* Schwinger model, in which $m_0 = 0$. The continuum model is exactly solvable and equivalent to a *massive* free bosonic model [45]. This makes it particularly appealing as a test case, as the whole spectrum of the theory is known analytically. Notably, the first excited state has a mass of $m_{\text{gap}} = g/\sqrt{\pi}$ or conversely a correlation length of $\xi \sim \sqrt{\pi}/g$. This gives an estimate of how much correlation needs to be built-into the system and how large a system is needed to correctly capture the infinite volume system. The correlation length gives an approximate estimate of how far interactions typically extend. If the physical volume, here the length N_s, is too small compared to correlation length, then there will be noticeable self interaction effects or boundary contamination. Thus a sufficiently large volume is one that is multiple times the correlation length of the system.

III. EXISTING METHODS

The VQE [14] is a state preparation algorithm that begins with some initial state $|\psi_{\text{ref}}\rangle$ which is trivial to initialize on a quantum computer, and then constructs an optimal trial state $|\psi\rangle = \hat{U}(\vec{\theta})|\psi_{\text{ref}}\rangle$, where $\hat{U}$ is a unitary operator encoded by a quantum circuit parameterized by angles $\vec{\theta}$. A classical optimization is used to find the ideal choice of angles that minimize some objective function. For example, to prepare the ground state of a physical system the objective function can be the expectation value of the energy. In this paper we assume the latter whenever we refer to optimization. To be specific, our objective function is $E_\psi \equiv \langle\psi|H|\psi\rangle$, using the Hamiltonian of Eq. (1). We note that, especially for one-dimensional systems with finite entanglement entropy, an alternative objective function for designing scalable quantum circuits could be the overlap with the ground state of a classical surrogate, such as an MPS [154]. In this case one would use the fidelity of the target state, which might speed up the preparation of excited quantum states.

ADAPT-VQE [39] is an algorithm that iteratively extends and updates the unitary

$$\hat{U}^{(k)}(\vec{\theta}^{(k)}) = \prod_{j=1}^{k} e^{-i\theta_j^{(k)}\hat{O}_{i_j}}, \tag{2}$$

where each element $\theta_j^{(k)}$ of the parameter vector $\vec{\theta}^{(k)}$ is the coefficient corresponding to the operator $\hat{O}_{i_j}$ drawn from a predefined pool $\{\hat{O}_i\}$. Note that $\hat{U}^{(k)}$ encodes the entire circuit up to iteration k, where each θ_j is equivalent to a time over which the trial state is evolved under a Hamiltonian $\hat{O}_{i_j}$. In each iteration of ADAPT-VQE, the unitary $\hat{U}$ is extended with a new $\hat{O}_{i_{k+1}} \in \{\hat{O}_i\}$ using a "greedy" procedure, selecting that $\hat{O}_i$ which confers the largest gradient $|\partial E_\psi/\partial\theta_{k+1}|_{\vec{\theta}^{(k)}}$ of the objective function at the current optimized trial state. After appending the new operator, the variational parameters $\theta_j^{(k+1)}$ in the circuit are reoptimized, initializing the values $\theta_{j\leq k}$ with the optimized value from the previous iteration, and initializing θ_{k+1} to zero. Operators are appended and optimizations repeatedly, until the gradients corresponding to every candidate operator fall below some user-defined threshold ϵ, such that

$$\epsilon > \left|\frac{\partial E_\psi}{\partial\theta_{k+1}}\right|_{\vec{\theta}^{(k)}_{\text{converged}}}, \tag{3}$$

for all choices $\hat{O}_{i_{k+1}} \in \{\hat{O}_i\}$. Note that the ADAPT-VQE convergence criterion, ϵ, is independent of, and typically larger than, the convergence criterion used to terminate each individual optimization.

For small molecules mapped to fewer than 14 qubits, this has been shown to yield highly compact ansätze and reach arbitrarily accurate energies [39].

While the original ADAPT-VQE algorithm used fermionic single- and double-excitations as the pool operators, there has been significant work to find optimal pool operator choices for ADAPT-VQE. For instance, Ref. [155] introduces the qubit-ADAPT operator pool, which breaks Jordan-Wigner-transformed fermionic excitations into individual terms, and drops Z-operators to make them more hardware-efficient. Ref. [156] introduces qubit-excitation based operators, another hardware-efficient construction in which Z-operator strings are removed from the Jordan-Wigner-transformed fermionic excitations. Ref. [157] discusses symmetry-adapted operators that incorporate problem symmetries such as the conservation of spin, particle number, and the point-group. Ref. [42] introduces operator tiling for translation-symmetric systems, tiling problem-relevant Pauli operators chosen by ADAPT-VQE across the entire system. Ref. [158] introduces Coupled Exchange Operators which create linear combinations of qubit-excitation operators acting on the same set of spin-orbitals.

Of particular interest to high energy and nuclear physics are the Scalable-Circuits ADAPT-VQE (SC-ADAPT-VQE) for extrapolating ansätze from small to large systems [28, 31]. This method adopts a pool of coordinate-invariant operators, so that circuits trained on a series of classical ADAPT-VQE simulations at small volumes can be scaled to those at large volumes, which are then run on a quantum computer. This obviates the need for running ADAPT-VQE or even VQE to obtain optimized parameters on a large volume, since the parameters are obtained via fitting and extrapolation from smaller systems. The operator pool for ADAPT-VQE is arbitrary, in principle, but judicious choices for the pool operators can improve convergence. The operator pool used in Ref. [28] for running ADAPT-VQE on the Schwinger model Hamiltonian in Eq. (1), which we will

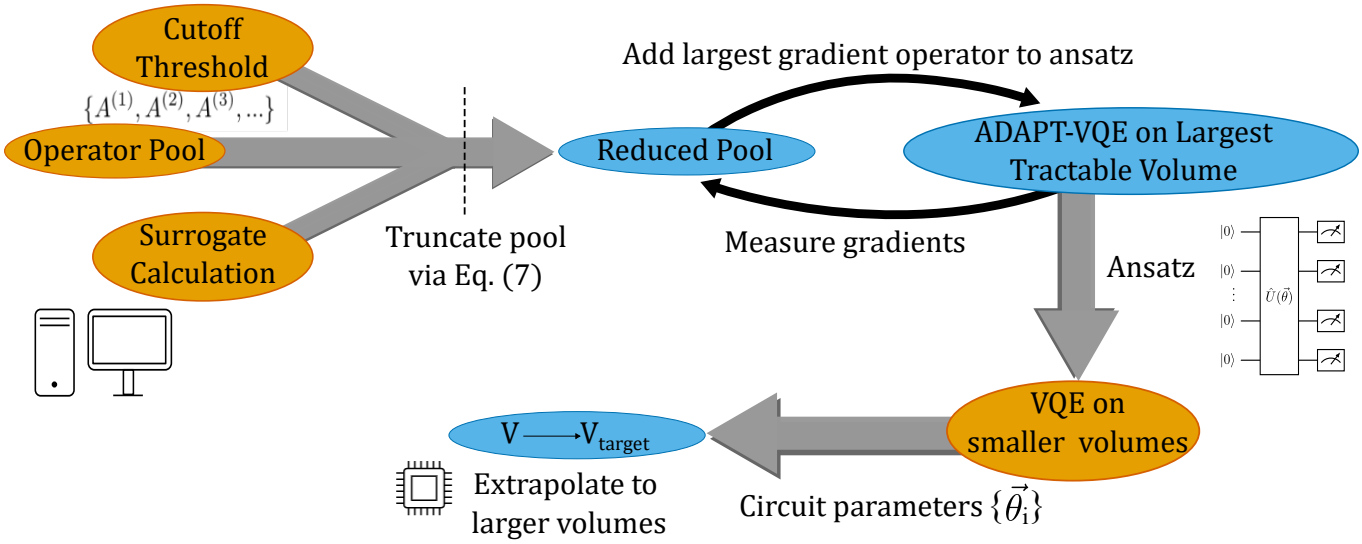

FIG. 1. Flow chart describing the $(SC)^2$-ADAPT-VQE work flow. Blue components indicate the workflow with (SC-)ADAPT-VQE [28, 31] while orange components those added with $(SC)^2$-ADAPT-VQE. The surrogate calculations along with a cutoff threshold, Δ come together to give a rigorous definition of a truncated operator pool. The reduced pool is utilized in an ADAPT-VQE calculation at the largest volume that can be simulated on a classical computer. This ansatz is then optimized on smaller volumes. If so desired, the resulting parameters $\{\vec{\theta}_i\}$ can then be extrapolated to larger volumes on a quantum computer. The thin black arrows illustrate that the classical adaptive part of ADAPT-VQE iteratively constructs a quantum circuit, using operators sampled from the truncated pool.

refer to as the *full singles* pool, includes

$$\hat{O}^V_{mh}(d) = \sum_{n=0}^{N_s-1-d} (-1)^n \hat{O}^{(d)}_n, \tag{4a}$$

$$\hat{O}^S_{mh}(m,d) = \left(\hat{O}^{(d)}_m + \hat{O}^{(d)}_{N_s-m-1-d}\right), \tag{4b}$$

where

$$\hat{O}^{(d)}_n \equiv \frac{i}{2}\left(\hat{\sigma}^+_n \hat{Z}^d_n \hat{\sigma}^-_{n+d} - \text{h.c.}\right); \tag{4c}$$

$\hat{Z}^d_n \equiv \bigotimes_q \hat{Z}_q$ denotes a string operator of length $d-2$ acting on all sites q between σ^+_n and σ^-_{n+d}. The subscript with $\hat{O}_{mh}$ stands for the combined effect of *m*ass and *h*opping terms [28]. The superscripts V or S indicate that the operator is a volume (bulk) or surface (boundary) term, respectively. These terms respect the time reversal symmetry of the ground state of the model, and represent the insertion of a single meson of length d. While Eq. (4a) does so uniformly throughout the system, Eq. (4b) only does so at a distance m from the open boundaries. The latter is expected to be useful, as boundary effects will be critical regardless of the values of g and m_0. Of importance here is that the operator pool construction leads to a different set of operators being available at each volume. When the ADAPT-VQE trajectory includes all new pool operators appearing at each volume, robustly extrapolating the sequence of operators becomes non-trivial.

The insertion of single meson is like the singles term in a unitary coupled cluster (UCC) ansatz. When including all permissible d and m for a given system size N_s in Eqs. (4), henceforth we refer to this as the *full singles pool*. This method can be extended to include an ansatz which inserts two mesons which do not overlap, or double terms [14, 159] which are of the form $i\hat{a}^\dagger_j \hat{a}_{j+d} \hat{a}^\dagger_k \hat{a}_{k+d'} - h.c.$. For the parameters we studied, however, we found that the contribution of such two meson operators was negligible. It is not clear if this is true in general, especially for models that possess many internal degrees of freedom. One notable example is that of multiple flavors of quarks in quantum chromodynamics.

IV. $(SC)^2$-ADAPT-VQE

Our algorithm, which we term Surrogate-Constructed Scalable-Circuits ADAPT-VQE, or $(SC)^2$-ADAPT-VQE, uses a classically tractable *surrogate* theory to select a subset of relevant operators in the ADAPT-VQE operator pool, independent of volume. This procedure defines a new, *truncated* pool, and a *minimum volume* for which *any* ADAPT-VQE circuit built from the truncated pool is well-defined. Therefore, we construct an ansatz just once, by running a classical ADAPT-VQE simulation with the truncated pool on the largest tractable volume. To generate a series of circuits from which to extrapolate to an even larger volume simulable with a quantum computer, we run classical VQE simulations *with a consistent ansatz* on each smaller volume, down to the minimum volume defined by the truncated pool. The high level flow chart for this algorithm is illustrated in Fig. 1.

The surrogate theory can widely vary, but it should be

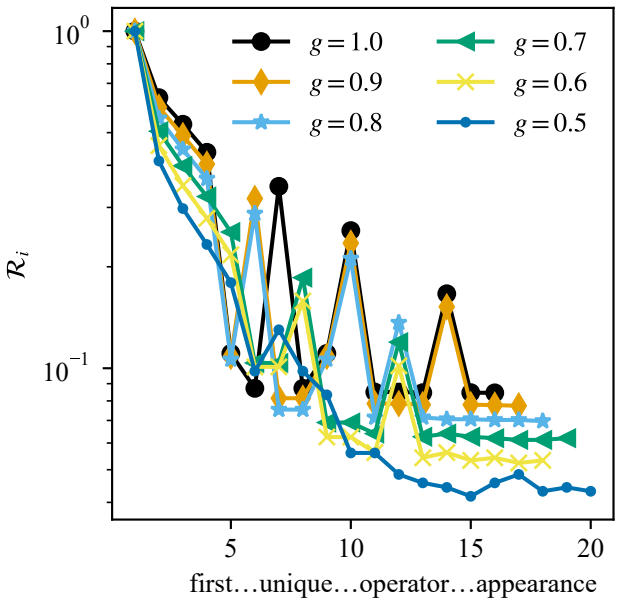

FIG. 2. Scaling of the transition matrix element operator, $\mathcal{R}_i$, versus the order the operator first uniquely appears in ADAPT-VQE applied to the massless Schwinger model, using the pool in Eq. 4 on lattices with $N_s = 16$ and various couplings g as specified in the legend. Operators that appear later suggest that they are less relevant to the state preparation. We see that it indeed does strongly correlate with $\mathcal{R}_i$.

accurate, reasonably scalable, systematically improvable, and calculable efficiently at the classical level. Examples of such surrogate theories could include coupled cluster calculations, matrix product states, sparse wavefunction simulators, and Markov chain Monte Carlo. The first step of (SC)^2-ADAPT-VQE uses a surrogate theory to measure the overlap operator

$$\mathcal{M}_j \equiv |\langle\psi_{\rm ref}|\hat{O}_j|\psi_{\rm sur}\rangle|^2. \tag{5}$$

In this equation $\hat{O}_j$ is the Hermitian operator that generates the rotations in Eq. (2), and $|\psi_{\rm sur}\rangle$ is an approximation of the ground state that might be determined classically. This can be done in several ways: in $1+1$ dimensions, using the density matrix renormalization group, or for higher dimensions, with projected pair entangled states. Lastly, $|\psi_{\rm ref}\rangle$ is an initial state that is easy to prepare. Here we use the strong coupling limit for the Schwinger model ($g \to \infty$), $|\psi_{\rm ref}\rangle = |0101.....01\rangle$. In chemistry problems one might use the Hartree-Fock state for $|\psi_{\rm ref}\rangle$. The values $\mathcal{M}_j$ are calculated only once for a choice of couplings (g, m_0) before any ADAPT-VQE calculations are run. In particular it is worth noting that the states themselves $|\psi_{\rm sur}\rangle$ and $|\psi_{\rm ref}\rangle$ do not need to be calculated explicitly, only the transition matrix element $\mathcal{M}_j$.

This operator is similar to a transition matrix element as it is the square of the linear term in the Maclaurin series approximation of $\langle\psi_{\rm ref}|e^{-i\theta\hat{O}_j}|\psi_{\rm sur}\rangle$, up to an overall constant. This choice of operator is reasonably well founded as it forms an approximation for the leading order contribution to a Maclaurin series expansion of the target operator. This transition matrix element is calculated classically. Next we impose a cut-off Δ such that we only keep operators $\hat{O}_j$ that satisfy

$$\mathcal{R}_j \equiv \frac{|\mathcal{M}_j|}{\max(|\mathcal{M}_{\rm j}|)} \geq \Delta. \tag{6}$$

While the fixed choice of the cut-off, Δ, is arbitrary, it allows for a consistent algorithmic construction of the operator pool, by removing possible biases at a given choice in parameter space. As Δ is taken to smaller values the size of the operator pool increases.

The operators chosen in standard ADAPT-VQE, and the scaling of $\mathcal{R}_j$, are correlated, as illustrated in Fig. 2. We find that the MPS amplitudes behave in a reasonably correlated manner with respect to the order of their first appearance in the ADAPT-VQE ansatz.

One source of instability in SC-ADAPT-VQE is the relatively large volume needed to obtain a consistent operator sequence in each run of ADAPT-VQE. This is illustrated for $g = 1.0$ and $m_0 = 0$ in Fig. 3 for both the truncated ($\Delta > 10^{-5}$) and full singles ($\Delta = 0$) operator pool. The figure uses shaded boxes to indicate different operators in the circuit: the grey operators correspond to the volume operators, $\hat{O}^V_{mh}(d)$, while the blue and orange regions correspond to the surface or boundary operators, $\hat{O}^S_{mh}(m,d)$. While operators with an early depth, *i.e.* the first through eighth, stabilize by $N_s = 12$, at this point the later operators have not stabilized. This implies that for progressively deeper (more accurate) ansätze, one needs progressively larger classical calculations to find a quantum circuit with an appropriately large volume. Crucially, we observe that the presence of different operators later on, which are needed for ADAPT to converge, still results in erratic behavior for the parameters ofof those early operators. Using the ansatz for $10 \leq N_s \leq 16$, we show mild non-monotonicity for the optimization angles for the first three operators in Fig. 4. With (SC)^2-ADAPT-VQE, we immediately start with the largest volume at which we can simulate classically, which we fix at $N_s = 16$. We use this ansatz to set the operator ordering, and then, where feasible, use the same circuit structure at smaller volumes. Doing so, we find that the optimized parameters exhibit increased monotonicity. One feature of note is that given the various operators $\hat{O}^V_{mh}(d)$ are themselves Trotterized, it is possible for ADAPT-VQE to select the same operator multiple times which might not typically happen in non-lattice systems.

An obvious limitation of (SC)^2-ADAPT-VQE is the capabilities of the surrogate theory. This has to be kept in mind particularly for critical systems, or when taking the continuum limit, as then the correlation length of the system, in units of the lattice spacing, diverges. This places limits on the range of parameters directly ac-

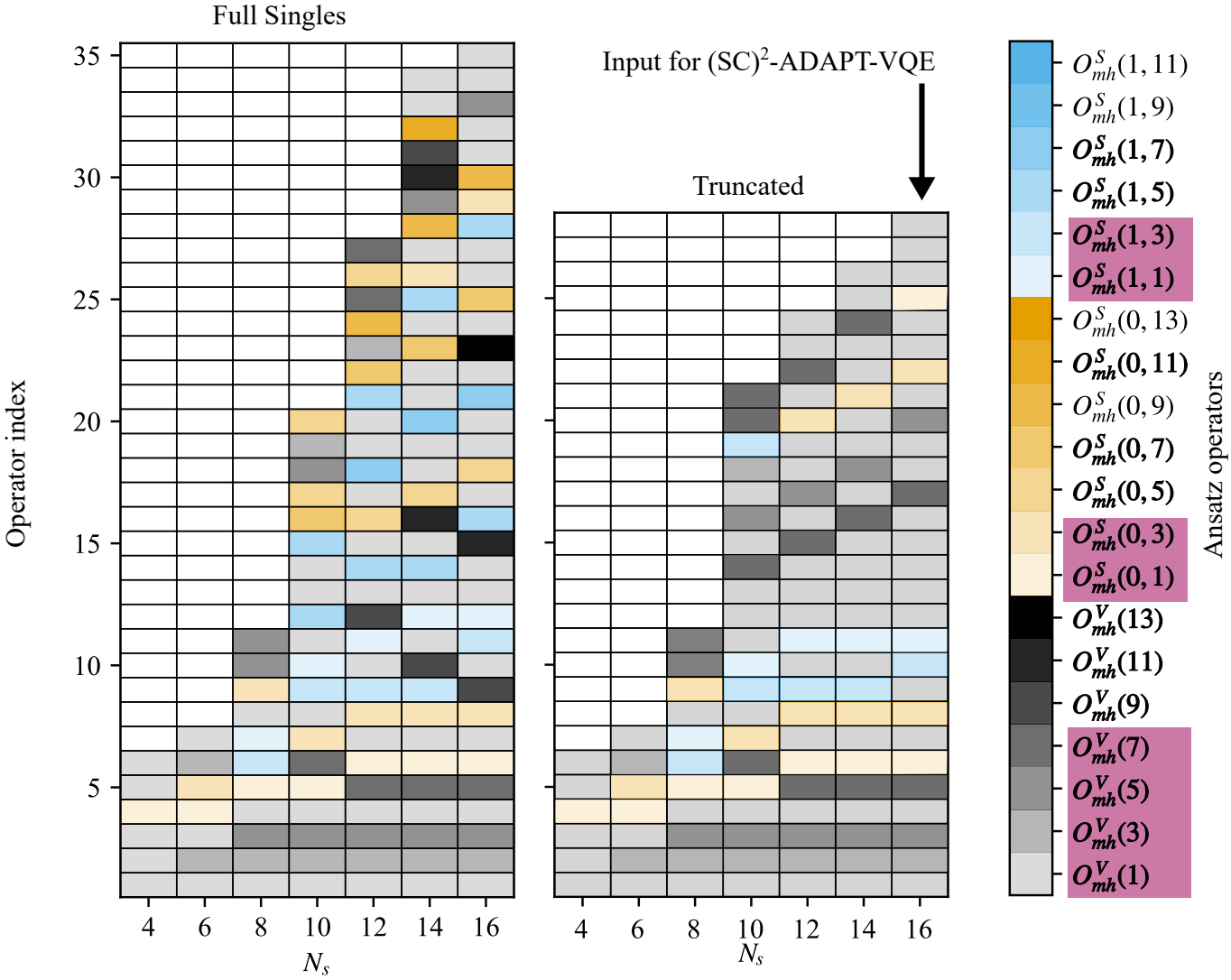

FIG. 3. Ansatz order for the full singles pool (left) and the truncated pool (right), using ADAPT-VQE with $g = 1.0$ and $m_0 = 0.0$. These simulations used the gradient convergence criterion of $\epsilon = 10^{-3}$, Eq. (3). The operators are defined in Eq. (4), while the legend to the right is the full singles pool for $N_s = 16$. Bold-face in the legend indicates that the operator was selected by ADAPT-VQE using the full singles pool for at least one volume. The magenta highlighting indicates which operators were chosen for the truncated pool with $\Delta = 10^{-5}$. The different colors denote different types of operators that appear in the ansatz. Volume operators are shaded from grey to black as their length increases. Orange denotes surface operators that touch the edge of the lattice, while blue operators are one lattice site from the edge. Notice that there is a striking regularity of the operators which persist as N_s increases for the surrogate truncated pool, versus that of the full singles pool. This demonstrates the utility of our truncation method.

cessible from a given surrogate. Alternatively, it places constraints on the type of surrogates that should be used.

V. RESULTS

While constructing a gauge theory on a lattice is a useful computational tool, eventually we are interested in the continuum limit. Since the product of the lattice spacing times the gauge coupling, ag, is dimensionless, at fixed lattice spacing a we can approach the continuum limit by taking $g \to 0$. In doing so, the ratio of m_0/g is held fixed, with different values corresponding to distinct theories.

In this section we show how results using (SC)^2-ADAPT-VQE can be used to reliably extrapolate to the continuum limit for the massless theory. While usually this is the most challenging case, for the special case of the Schwinger model the model is solvable analytically, with the spectrum only a single free, massive boson. As a fiducial quantity, we compute the expectation value of

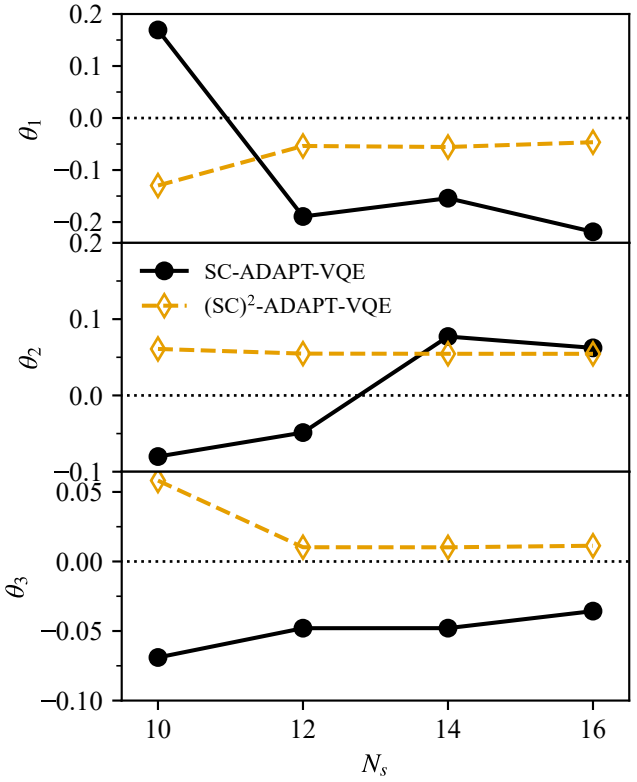

FIG. 4. Optimized coefficients θ_j for the first (top), second (middle), and third (operator) selected by ADAPT-VQE applied to the massless Schwinger model with $ag = 1.0$. For the SC-ADAPT-VQE curve (solid), ADAPT-VQE was solved at each volume using the pool in Eq. 4, up to a gradient convergence criterion of $\epsilon = 10^{-3}$. For the (SC)^2-ADAPT-VQE curve (dashed), ADAPT-VQE was solved at a volume of $N_s = 16$ up to the same ϵ and using the same pool, but truncated according to Eq. 6 with $\Delta = 10^{-5}$. The resulting circuit was re-optimized for volumes $N_s < 16$. All runs of ADAPT-VQE selected the same first three operators, irrespective of volume ($O^V_{mh}(1)$ for θ_1, $O^V_{mh}(3)$ for θ_2, $O^V_{mh}(5)$ for θ_3). However, the SC-ADAPT-VQE runs at different volumes selected different operators later on in the ansatz. This produced an extreme non-monotonicity in the optimized coefficients, and so an ambiguous extrapolation to the limit of infinite volume. The (SC)^2-ADAPT-VQE protocol resolves this problem.

the chiral condensate,

$$\langle\bar{\psi}\psi\rangle = \frac{1}{2N_s}\sum_{j=0}^{N_s-1}(-1)^j\langle\hat{\sigma}^z_j\rangle. \tag{7}$$

This expectation value is trivially nonzero when there is a fermion mass. However, it remains non-zero even if $m_0 \to 0$. There, spontaneous dimerization of the system occurs dynamically, with the analytical continuum limit given by[160]

$$\langle\bar{\psi}\psi\rangle_0 \;=\; -\frac{g}{2\pi^{3/2}}e^{\gamma_E} \qquad (m_0 = 0) \tag{8}$$

with $\gamma_E = 0.5772$ the Euler constant.

TABLE I. Characteristic numbers for (SC)^2-ADAPT-VQE applied to the massless Schwinger model, using pools constructed from Eqs. 4 and 6 with different values of Δ. The "Depth" columns identify the number of operators selected by ADAPT-VQE at a volume of $N_s = 16$ up to a gradient convergence criterion of $\epsilon = 10^{-3}$. The "Min N_s" columns identify the minimum volumes for which all operators in the pool are defined. Without truncation (i.e. using $\Delta = 0$), there is no well-defined minimum N_s.

	Full singles ($\Delta = 0$)	Truncated ($\Delta = 10^{-5}$)		Heavily truncated ($\Delta = 10^{-3}$)	
ag	Depth	Depth	Min N_s	Depth	Min N_s
1.0	34	27	10	22	6
0.9	32	27	10	23	6
0.8	35	27	10	22	6
0.7	31	32	12	32	8
0.6	33	36	12	30	8
0.5	37	36	14	32	10

We choose to compute $\langle\bar{\psi}\psi\rangle$ rather than just the energy (which serves as the objective function in our ADAPT-VQE calculations), as it receives contributions from off-diagonal elements in the energy eigenbasis, and so provides a better measure of accuracy.

Before proceeding to the continuum limit, it is important to investigate aspects of the operator pool truncation at finite volumes and non-zero lattice spacings. Fig. 5 shows the relative error of the chiral condensate at $m_0 = 0$ and $g = 0.7$, of distinct ADAPT-VQE trial states constructed independently for each volume, using three fiducial values of the threshold Δ for $\mathcal{R}_j$: $\Delta = 0$, 10^{-5}, and 10^{-3}, which we denote as the full singles, truncated, and heavily truncated operator pools, respectively. For sufficiently small volumes there is no significant difference between the three truncations. By a volume of $N_s = 14$, though, significant discrepancies arise, and it is clear that there are "truncation" artifacts that become noticeably important. The deviations grow weakly towards larger volumes where certain operators transition from being irrelevant to important. These cases will become more prevalent when the gradient truncation threshold ϵ is decreased, and volume artifacts begin to stabilize.

We are now in a position to investigate how truncating the operator pool affects calculations in the thermodynamic and continuum limits. In Fig. 6, we perform the (SC)^2-ADAPT-VQE procedure (solving ADAPT-VQE at just one volume for each coupling parameter) for the truncated and heavily truncated pools to obtain estimates of the chiral condensate in the thermodynamic limit. As a control, we compare against the SC-ADAPT-VQE procedure (solving ADAPT-VQE for each volume) with the full singles pool. Note that for these results, we extrapolate the observable directly, rather than the operator coefficients, to sidestep the instabilities observed in Fig. 4.

Using the thermodynamic limit values for each coupling parameter, we then perform another extrapolation

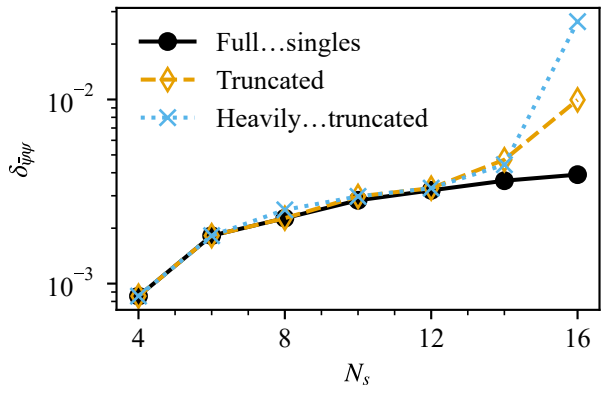

FIG. 5. Relative error $\delta_{\bar{\psi}\psi} \equiv |\langle\bar{\psi}\psi\rangle - \langle\bar{\psi}\psi\rangle_0|/|\langle\bar{\psi}\psi\rangle_0|$ of chiral condensates obtained from $(SC)^2$-ADAPT-VQE applied to the massless lattice Schwinger model with $ag = 0.7$ using Eq. (8). ADAPT-VQE was solved at each volume up to a gradient convergence criterion of $\epsilon = 10^{-3}$. Each curve used a distinct pool, constructed from Eqs. (4) and (6) with $\Delta = 0$ (full singles), 10^{-5} (truncated), and 10^{-3} (heavily truncated). Chiral condensates for each optimized circuit were measured, and their relative error was calculated with respect to DMRG calculations of matching volume, with a maximal bond dimension of 400.

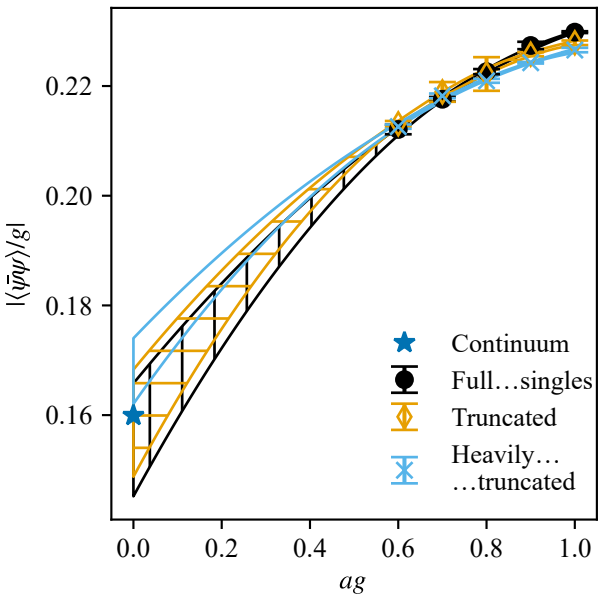

FIG. 6. Chiral condensates obtained from $(SC)^2$-ADAPT-VQE applied to the massless lattice Schwinger model, with an extrapolation to the continuum limit. Each curve used a distinct pool, constructed from Eqs. 4 and 6 with $\Delta = 0$ (full singles), 10^{-5} (truncated), and 10^{-3} (heavily truncated). In the truncated and heavily truncated curves, ADAPT-VQE was solved for each parameter value ag at a volume of $N_s = 16$ up to a gradient convergence criterion of $\epsilon = 10^{-3}$, and the resulting circuits were re-optimized for volumes $N_s < 16$, down to the minimum volumes given in Table I. Because there is no defined minimum volume for the full singles pool, ADAPT-VQE was solved independently for each volume $4 \leq N_s \leq 16$. Chiral condensates for each optimized circuit were measured, and extrapolated to the thermodynamic ($N_s \to \infty$) limit, yielding the points seen in the plot. The errorbars with the symbols derive from systematic errors occurring from the infinite volume extrapolations. The shaded areas show an extrapolation to the continuum limit ($a \to 0$) as the confidence interval of the underlying polynomial fit. The asterisk at $ag = 0$ represents the exact analytic result, Eq. (8) for $g = 1$. This demonstrates that the truncation of the operator pool has minimal effect on the final continuum limits.

to the continuum limit. For $g = 1$, from Eq. (8) the result in the continuum limit is $\langle\bar{\psi}\psi\rangle_0 = -0.159929$. Using $(SC)^2$-ADAPT-VQE with a truncated pool, the result we find after taking $ag \to 0$, indicated by the blue asterisk in Fig. 6, agrees well with this result. This demonstrates that while certain marginal operators may appear in the full ADAPT-VQE pool, that at least for the value of the chiral condensate, in practice their effect is minimal. This robustness encourages using $(SC)^2$-ADAPT-VQE to reach the continuum limit in this and other field theories.

VI. OUTLOOK

We have developed an algorithm, $(SC)^2$-ADAPT-VQE, which addresses certain ambiguities in the SC-ADAPT-VQE algorithm of Ref. [28]. This method utilizes classically scalable resources to efficiently identify an operator pool which is well-defined on any number of qubits above a minimum volume. This allows a single classical execution of ADAPT-VQE to generate a fixed ansatz which can be optimized via VQE for smaller volumes, providing a robust sequence of parameters that can be extrapolated to large volumes executable on quantum hardware. We also note the reduced operator pool can reduce the overall sampling budget by a factor linear in the size of the system. We have not examined our extensions to the algorithm at scale on a quantum computer because the noise on present day devices prohibitively accumulates for the long circuit depths we consider. Nevertheless, this improvement to the algorithm greatly stabilizes extrapolating to larger, scalable circuits. This is crucial for looking at theories with long correlation lengths, especially as arises in approaching the continuum limit. In particular when we want to expand to larger systems, the choice of Δ can depend on the process, observable, and model or theory. Therefore, it will be important to develop other theory-specific heuristics that might improve upon or replace the choice procedure of the cutoff.

We have demonstrated that $(SC)^2$-ADAPT-VQE can be used to approach the continuum limit of relativistic field theories, using the Schwinger model as an example. This makes it a promising method for state preparation of near-term quantum simulations of a variety of low-

dimensional models, including the multi-flavor Schwinger model [45], QCD_2 [161], and even bosonic models such as $\lambda\phi^4$ [162] and the Abelian-Higgs model [163]. A particularly interesting prospect would be useful to apply this method to QZD, a $Z(3)$ gauge theory coupled to three flavors of fermions [164]. This model has both confined fermions and bosons, analogous to the baryons and mesons of QCD. Like QCD, cold, dense QZD has a severe sign problem. Using $(SC)^2$-ADAPT-VQE to study QZD will be of use both to investigate the Fermi sea of the theory, as well as to understand how $(SC)^2$-ADAPT-VQE behaves in the presence of more complicated excitations.

The increase in correlation length of the system as the continuum is approached is only a specific example of a system going through a second-order phase transition. As such, $(SC)^2$-ADAPT-VQE also poses itself as an ideal algorithm to address the issue of ground state preparation of critical systems, close to and away from quantum phase transitions. This includes many models in condensed matter physics, such as the Hubbard model.

In ADAPT-VQE simulations of molecular systems utilizing Gaussian basis sets, one could easily utilize portions of the $(SC)^2$-ADAPT-VQE algorithm for the operator pool selection component. In particular this method should be able to reduce the number of possible operators for an UCC type ansatz, which is useful in electronic systems.

ACKNOWLEDGMENTS

The authors thank Anthony Ciavarelli, Roland Farrell, Marc Illa, Abid Kahn, Wayne J. Mullinax, Martin Savage, and Nikita Zemlevskiy for helpful comments. K. Sherbert, A.F., K. Shirali, Y.C., S.V., A. W., S.E.E., R.D.P., and N.M.T. are supported by the U.S. Department of Energy, Office of Science, National Quantum Information Science Research Centers, Co-design Center for Quantum Advantage (C^2QA) under Contract No. DE-SC0012704. C^2QA led this research. E.G. was supported by the NASA Academic Mission Services, Contract No. NNA16BD14C and NASA-DOE interagency agreement SAA2-403602. A.F. and R.D.P. were supported by the U.S. Department of Energy under contract DE-SC0012704. H.L. and E.G., are supported by the U.S. Department of Energy, Office of Science, National Quantum Information Science Research Centers, Superconducting Quantum Materials and Systems Center (SQMS) under contract number DE-AC02-07CH11359. Fermilab is operated by Fermi Research Alliance, LLC under contract number DE-AC02-07CH11359 with the United States Department of Energy. S.V. was supported by the U.S. Department of Energy, Nuclear Physics Quantum Horizons program through the Early Career Award DE-SC0021892. A.W. was supported by the U.S. Department of Energy, Office of Science, Basic Energy Sciences, Materials Sciences and Engineering Division. The authors acknowledge use of the HSL4 computing system for larger scale simulations. This research used resources of the National Energy Research Scientific Computing Center, a DOE Office of Science User Facility supported by the Office of Science of the U.S. Department of Energy using NERSC award ASCR-ERCAP0024469.

[1] B. Bauer, S. Bravyi, M. Motta, and G. K.-L. Chan, Quantum Algorithms for Quantum Chemistry and Quantum Materials Science, Chemical Reviews **120**, 12685 (2020), publisher: American Chemical Society.

[2] S. McArdle, S. Endo, A. Aspuru-Guzik, S. C. Benjamin, and X. Yuan, Quantum computational chemistry, Reviews of Modern Physics **92**, 015003 (2020).

[3] Y. Cao, J. Romero, J. P. Olson, M. Degroote, P. D. Johnson, M. Kieferová, I. D. Kivlichan, T. Menke, B. Peropadre, N. P. Sawaya, *et al.*, Quantum chemistry in the age of quantum computing, Chemical reviews **119**, 10856 (2019).

[4] D. Grabowska, Quantum simulations of lattice field theories, PoS **LATTICE2023**, 110 (2024).

[5] N. Klco, A. Roggero, and M. J. Savage, Standard model physics and the digital quantum revolution: thoughts about the interface, Rept. Prog. Phys. **85**, 064301 (2022), arXiv:2107.04769 [quant-ph].

[6] M. S. Alam *et al.*, Quantum computing hardware for HEP algorithms and sensing, in *2022 Snowmass Summer Study* (2022) arXiv:2204.08605 [quant-ph].

[7] R. P. Feynman, Simulating physics with computers, Int. J. Theor. Phys. **21**, 467 (1982).

[8] C. W. Bauer *et al.*, Quantum Simulation for High-Energy Physics, PRX Quantum **4**, 027001 (2023), arXiv:2204.03381 [quant-ph].

[9] A. Di Meglio *et al.*, Quantum Computing for High-Energy Physics: State of the Art and Challenges. Summary of the QC4HEP Working Group (2023), arXiv:2307.03236 [quant-ph].

[10] C. W. Bauer, Z. Davoudi, N. Klco, and M. J. Savage, Quantum simulation of fundamental particles and forces, Nature Rev. Phys. **5**, 420 (2023), arXiv:2404.06298 [hep-ph].

[11] K. Klymko, C. Mejuto-Zaera, S. J. Cotton, F. Wudarski, M. Urbanek, D. Hait, M. Head-Gordon, K. B. Whaley, J. Moussa, N. Wiebe, W. A. de Jong, and N. M. Tubman, Real-time evolution for ultracompact hamiltonian eigenstates on quantum hardware, PRX Quantum **3**, 020323 (2022).

[12] Y. Alexeev, M. Amsler, M. A. Barroca, S. Bassini, T. Battelle, D. Camps, D. Casanova, Y. J. Choi, F. T. Chong, C. Chung, *et al.*, Quantum-centric supercomputing for materials science: A perspective on chal-

lenges and future directions, Future Generation Computer Systems **160**, 666 (2024).
[13] A. Aspuru-Guzik, A. D. Dutoi, P. J. Love, and M. Head-Gordon, Simulated quantum computation of molecular energies, Science **309**, 1704 (2005), https://www.science.org/doi/pdf/10.1126/science.1113479.
[14] A. Peruzzo, J. McClean, P. Shadbolt, M.-H. Yung, X.-Q. Zhou, P. J. Love, A. Aspuru-Guzik, and J. L. O'brien, A variational eigenvalue solver on a photonic quantum processor, Nature communications **5**, 1 (2014).
[15] B. Bauer, D. Wecker, A. J. Millis, M. B. Hastings, and M. Troyer, Hybrid quantum-classical approach to correlated materials, Phys. Rev. X **6**, 031045 (2016).
[16] D. W. Berry, M. Kieferová, A. Scherer, Y. R. Sanders, G. H. Low, N. Wiebe, C. Gidney, and R. Babbush, Improved techniques for preparing eigenstates of fermionic hamiltonians, npj Quantum Information **4** (2018).
[17] X. Yuan, S. Endo, Q. Zhao, Y. Li, and S. C. Benjamin, Theory of variational quantum simulation, Quantum **3**, 191 (2019).
[18] N. M. Tubman, C. Mejuto-Zaera, J. M. Epstein, D. Hait, D. S. Levine, W. Huggins, Z. Jiang, J. R. McClean, R. Babbush, M. Head-Gordon, and K. B. Whaley, Postponing the orthogonality catastrophe: efficient state preparation for electronic structure simulations on quantum devices, arXiv e-prints , arXiv:1809.05523 (2018), arXiv:1809.05523 [quant-ph].
[19] M. Motta, C. Sun, A. T. Tan, M. J. O'Rourke, E. Ye, A. J. Minnich, F. G. Brandao, and G. K.-L. Chan, Determining eigenstates and thermal states on a quantum computer using quantum imaginary time evolution, Nature Physics **16**, 205 (2020).
[20] N. Gomes, A. Mukherjee, F. Zhang, T. Iadecola, C.-Z. Wang, K.-M. Ho, P. P. Orth, and Y.-X. Yao, Adaptive variational quantum imaginary time evolution approach for ground state preparation, Advanced Quantum Technologies **4**, 2100114 (2021).
[21] J. B. Larsen, M. D. Grace, A. D. Baczewski, and A. B. Magann, Feedback-based quantum algorithms for ground state preparation, arXiv e-prints , arXiv:2303.02917 (2023), arXiv:2303.02917 [quant-ph].
[22] E. J. Gustafson, J. Tiihonen, D. Chamaki, F. Sorourifar, J. W. Mullinax, A. C. Y. Li, F. B. Maciejewski, N. P. Sawaya, J. T. Krogel, D. E. B. Neira, and N. M. Tubman, Surrogate optimization of variational quantum circuits (2024), arXiv:2404.02951 [quant-ph].
[23] A. Khan, P. Vaish, Y. Pang, N. Kowshik, M. S. Chen, C. H. Batton, G. M. Rotskoff, J. W. Mullinax, B. K. Clark, B. M. Rubenstein, and N. M. Tubman, Quantum Hardware-Enabled Molecular Dynamics via Transfer Learning, arXiv e-prints , arXiv:2406.08554 (2024), arXiv:2406.08554 [physics.chem-ph].
[24] C. Kokail *et al.*, Self-verifying variational quantum simulation of lattice models, Nature **569**, 355 (2019), arXiv:1810.03421 [quant-ph].
[25] E. J. Gustafson and H. Lamm, Toward quantum simulations of $\mathbb{Z}_2$ gauge theory without state preparation, Phys. Rev. D **103**, 054507 (2021), arXiv:2011.11677 [hep-lat].
[26] F. Turro, A. Roggero, V. Amitrano, P. Luchi, K. A. Wendt, J. L. DuBois, S. Quaglioni, and F. Pederiva, Imaginary-time propagation on a quantum chip, Phys. Rev. A **105**, 022440 (2022), arXiv:2102.12260 [quant-ph].
[27] A. N. Ciavarella and I. A. Chernyshev, Preparation of the SU(3) lattice Yang-Mills vacuum with variational quantum methods, Phys. Rev. D **105**, 074504 (2022), arXiv:2112.09083 [quant-ph].
[28] R. C. Farrell, M. Illa, A. N. Ciavarella, and M. J. Savage, Scalable circuits for preparing ground states on digital quantum computers: The schwinger model vacuum on 100 qubits, PRX Quantum **5**, 020315 (2024).
[29] R. Belyansky, S. Whitsitt, N. Mueller, A. Fahimniya, E. R. Bennewitz, Z. Davoudi, and A. V. Gorshkov, High-Energy Collision of Quarks and Mesons in the Schwinger Model: From Tensor Networks to Circuit QED, Phys. Rev. Lett. **132**, 091903 (2024), arXiv:2307.02522 [quant-ph].
[30] K. Lee, J. Mulligan, F. Ringer, and X. Yao, Liouvillian dynamics of the open Schwinger model: String breaking and kinetic dissipation in a thermal medium, Phys. Rev. D **108**, 094518 (2023), arXiv:2308.03878 [quant-ph].
[31] R. C. Farrell, M. Illa, A. N. Ciavarella, and M. J. Savage, Quantum Simulations of Hadron Dynamics in the Schwinger Model using 112 Qubits (2024), arXiv:2401.08044 [quant-ph].
[32] Z. Li, D. M. Grabowska, and M. J. Savage, Sequency Hierarchy Truncation (SeqHT) for Adiabatic State Preparation and Time Evolution in Quantum Simulations, (2024), arXiv:2407.13835 [quant-ph].
[33] F. Turro, A. Ciavarella, and X. Yao, Classical and quantum computing of shear viscosity for (2+1)D SU(2) gauge theory, Phys. Rev. D **109**, 114511 (2024), arXiv:2402.04221 [hep-lat].
[34] J. R. McClean, J. Romero, R. Babbush, and A. Aspuru-Guzik, The theory of variational hybrid quantum-classical algorithms, New Journal of Physics **18**, 023023 (2016).
[35] M. Cerezo, A. Arrasmith, R. Babbush, S. C. Benjamin, S. Endo, K. Fujii, J. R. McClean, K. Mitarai, X. Yuan, L. Cincio, *et al.*, Variational quantum algorithms, Nature Reviews Physics , 1 (2021).
[36] J. Tilly, H. Chen, S. Cao, D. Picozzi, K. Setia, Y. Li, E. Grant, L. Wossnig, I. Rungger, G. H. Booth, and J. Tennyson, The Variational Quantum Eigensolver: A review of methods and best practices, Physics Reports The Variational Quantum Eigensolver: a review of methods and best practices, **986**, 1 (2022).
[37] D. A. Fedorov, B. Peng, N. Govind, and Y. Alexeev, Vqe method: A short survey and recent developments, Materials Theory **6**, 1 (2022).
[38] A. Khan, B. K. Clark, and N. M. Tubman, Pre-optimizing variational quantum eigensolvers with tensor networks, arXiv e-prints , arXiv:2310.12965 (2023), arXiv:2310.12965 [quant-ph].
[39] H. R. Grimsley, S. E. Economou, E. Barnes, and N. J. Mayhall, An adaptive variational algorithm for exact molecular simulations on a quantum computer, Nature Commun. **10**, 3007 (2019), arXiv:1812.11173 [quant-ph].
[40] H. R. Grimsley, G. S. Barron, E. Barnes, S. E. Economou, and N. J. Mayhall, Adaptive, problem-tailored variational quantum eigensolver mitigates rough parameter landscapes and barren plateaus, npj Quantum Information **9**, 10.1038/s41534-023-00681-0 (2023).
[41] D. Z. Manrique, I. T. Khan, K. Yamamoto, V. Wichitwechkarn, and D. M. Ramo, Momentum-space uni-

tary coupled cluster and translational quantum subspace expansion for periodic systems on quantum computers (2021), arXiv:2008.08694 [quant-ph].
[42] J. S. Van Dyke, K. Shirali, G. S. Barron, N. J. Mayhall, E. Barnes, and S. E. Economou, Scaling adaptive quantum simulation algorithms via operator pool tiling, Phys. Rev. Res. **6**, L012030 (2024).
[43] J. S. Schwinger, Gauge Invariance and Mass. 2., Phys. Rev. **128**, 2425 (1962).
[44] S. R. Coleman, R. Jackiw, and L. Susskind, Charge Shielding and Quark Confinement in the Massive Schwinger Model, Annals Phys. **93**, 267 (1975).
[45] S. R. Coleman, More About the Massive Schwinger Model, Annals Phys. **101**, 239 (1976).
[46] E. J. Gustafson, H. Lamm, F. Lovelace, and D. Musk, Primitive quantum gates for an SU(2) discrete subgroup: Binary tetrahedral, Phys. Rev. D **106**, 114501 (2022), arXiv:2208.12309 [quant-ph].
[47] E. J. Gustafson, H. Lamm, and F. Lovelace, Primitive quantum gates for an SU(2) discrete subgroup: Binary octahedral, Phys. Rev. D **109**, 054503 (2024), arXiv:2312.10285 [hep-lat].
[48] M. S. Alam, S. Hadfield, H. Lamm, and A. C. Y. Li (SQMS), Primitive quantum gates for dihedral gauge theories, Phys. Rev. D **105**, 114501 (2022).
[49] Y. Ji, H. Lamm, and S. Zhu (NuQS), Gluon Field Digitization via Group Space Decimation for Quantum Computers, Phys. Rev. D **102**, 114513 (2020), arXiv:2005.14221 [hep-lat].
[50] T. Armon, S. Ashkenazi, G. García-Moreno, A. González-Tudela, and E. Zohar, Photon-Mediated Stroboscopic Quantum Simulation of a Z2 Lattice Gauge Theory, Phys. Rev. Lett. **127**, 250501 (2021), arXiv:2107.13024 [quant-ph].
[51] Y. Ji, H. Lamm, and S. Zhu (NuQS Collaboration), Gluon digitization via character expansion for quantum computers, Phys. Rev. D **107**, 114503 (2023).
[52] A. Alexandru, P. F. Bedaque, S. Harmalkar, H. Lamm, S. Lawrence, and N. C. Warrington (NuQS), Gluon field digitization for quantum computers, Phys.Rev.D **100**, 114501 (2019), arXiv:1906.11213 [hep-lat].
[53] A. Alexandru, P. F. Bedaque, R. Brett, and H. Lamm, Spectrum of digitized QCD: Glueballs in a S(1080) gauge theory, Phys. Rev. D **105**, 114508 (2022), arXiv:2112.08482 [hep-lat].
[54] C. Charles, E. J. Gustafson, E. Hardt, F. Herren, N. Hogan, H. Lamm, S. Starecheski, R. S. Van de Water, and M. L. Wagman, Simulating Z2 lattice gauge theory on a quantum computer, Phys. Rev. E **109**, 015307 (2024), arXiv:2305.02361 [hep-lat].
[55] E. M. Murairi, M. Sohaib Alam, H. Lamm, S. Hadfield, and E. Gustafson, Highly-efficient quantum Fourier transformations for some nonabelian groups (2024), arXiv:2408.00075 [quant-ph].
[56] E. J. Gustafson, Y. Ji, H. Lamm, E. M. Murairi, and S. Zhu, Primitive Quantum Gates for an SU(3) Discrete Subgroup: $\Sigma(36\times3)$ (2024), arXiv:2405.05973 [hep-lat].
[57] B. Assi and H. Lamm, Digitization and subduction of $SU(N)$ gauge theories (2024), arXiv:2405.12204 [hep-lat].
[58] H. Lamm, Y.-Y. Li, J. Shu, Y.-L. Wang, and B. Xu, Block Encodings of Discrete Subgroups on Quantum Computer (2024), arXiv:2405.12890 [hep-lat].
[59] I. Raychowdhury and J. R. Stryker, Solving Gauss's Law on Digital Quantum Computers with Loop-String-Hadron Digitization, Phys. Rev. Res. **2**, 033039 (2020), arXiv:1812.07554 [hep-lat].
[60] I. Raychowdhury and J. R. Stryker, Loop, String, and Hadron Dynamics in SU(2) Hamiltonian Lattice Gauge Theories, Phys. Rev. D **101**, 114502 (2020), arXiv:1912.06133 [hep-lat].
[61] Z. Davoudi, I. Raychowdhury, and A. Shaw, Search for efficient formulations for Hamiltonian simulation of non-Abelian lattice gauge theories, Phys. Rev. D **104**, 074505 (2021), arXiv:2009.11802 [hep-lat].
[62] S. V. Kadam, *Theoretical Developments in Lattice Gauge Theory for Applications in Double-beta Decay Processes and Quantum Simulation*, Ph.D. thesis, Maryland U., College Park (2023), arXiv:2312.00780 [hep-lat].
[63] E. Mathew and I. Raychowdhury, Protecting local and global symmetries in simulating (1+1)D non-Abelian gauge theories, Phys. Rev. D **106**, 054510 (2022), arXiv:2206.07444 [hep-lat].
[64] S. V. Kadam, A. Naskar, I. Raychowdhury, and J. R. Stryker, Loop-string-hadron approach to SU(3) lattice Yang-Mills theory: Gauge invariant Hilbert space of a trivalent vertex (2024), arXiv:2407.19181 [hep-lat].
[65] H. Liu and S. Chandrasekharan, Qubit Regularization and Qubit Embedding Algebras, Symmetry **14**, 305 (2022), arXiv:2112.02090 [hep-lat].
[66] R. Brower, S. Chandrasekharan, and U. J. Wiese, QCD as a quantum link model, Phys. Rev. D **60**, 094502 (1999), arXiv:hep-th/9704106.
[67] R. C. Brower, D. Berenstein, and H. Kawai, Lattice Gauge Theory for a Quantum Computer, PoS **LATTICE2019**, 112 (2019), arXiv:2002.10028 [hep-lat].
[68] S. Chandrasekharan and U. J. Wiese, Quantum link models: A Discrete approach to gauge theories, Nucl. Phys. **B492**, 455 (1997), arXiv:hep-lat/9609042 [hep-lat].
[69] J. Zhou, H. Singh, T. Bhattacharya, S. Chandrasekharan, and R. Gupta, Spacetime symmetric qubit regularization of the asymptotically free two-dimensional O(4) model, Phys. Rev. D **105**, 054510 (2022), arXiv:2111.13780 [hep-lat].
[70] N. Klco, E. F. Dumitrescu, A. J. McCaskey, T. D. Morris, R. C. Pooser, M. Sanz, E. Solano, P. Lougovski, and M. J. Savage, Quantum-classical computation of Schwinger model dynamics using quantum computers, Phys. Rev. **A98**, 032331 (2018), arXiv:1803.03326 [quant-ph].
[71] N. Klco, J. R. Stryker, and M. J. Savage, SU(2) non-Abelian gauge field theory in one dimension on digital quantum computers, Phys. Rev. D **101**, 074512 (2020), arXiv:1908.06935 [quant-ph].
[72] M. Illa, C. E. P. Robin, and M. J. Savage, Qu8its for Quantum Simulations of Lattice Quantum Chromodynamics (2024), arXiv:2403.14537 [quant-ph].
[73] A. Ciavarella, N. Klco, and M. J. Savage, Trailhead for quantum simulation of SU(3) Yang-Mills lattice gauge theory in the local multiplet basis, Phys. Rev. D **103**, 094501 (2021), arXiv:2101.10227 [quant-ph].
[74] A. Bazavov, Y. Meurice, S.-W. Tsai, J. Unmuth-Yockey, and J. Zhang, Gauge-invariant implementation of the Abelian Higgs model on optical lattices, Phys. Rev. **D92**, 076003 (2015), arXiv:1503.08354 [hep-lat].
[75] J. Zhang, J. Unmuth-Yockey, J. Zeiher, A. Bazavov,

S. W. Tsai, and Y. Meurice, Quantum simulation of the universal features of the Polyakov loop, Phys. Rev. Lett. **121**, 223201 (2018), arXiv:1803.11166 [hep-lat].

[76] A. Bazavov, S. Catterall, R. G. Jha, and J. Unmuth-Yockey, Tensor renormalization group study of the nonabelian higgs model in two dimensions, Phys. Rev. D **99**, 114507 (2019).

[77] C. W. Bauer and D. M. Grabowska, Efficient Representation for Simulating U(1) Gauge Theories on Digital Quantum Computers at All Values of the Coupling (2021), arXiv:2111.08015 [hep-ph].

[78] D. M. Grabowska, C. Kane, B. Nachman, and C. W. Bauer, Overcoming exponential scaling with system size in Trotter-Suzuki implementations of constrained Hamiltonians: 2+1 U(1) lattice gauge theories (2022), arXiv:2208.03333 [quant-ph].

[79] A. J. Buser, T. Bhattacharya, L. Cincio, and R. Gupta, Quantum simulation of the qubit-regularized O(3)-sigma model (2020), arXiv:2006.15746 [quant-ph].

[80] T. Bhattacharya, A. J. Buser, S. Chandrasekharan, R. Gupta, and H. Singh, Qubit regularization of asymptotic freedom (2020), arXiv:2012.02153 [hep-lat].

[81] A. H. Z. Kavaki and R. Lewis, From square plaquettes to triamond lattices for SU(2) gauge theory (2024), arXiv:2401.14570 [hep-lat].

[82] G. Calajò, G. Magnifico, C. Edmunds, M. Ringbauer, S. Montangero, and P. Silvi, Digital quantum simulation of a (1+1)D SU(2) lattice gauge theory with ion qudits (2024), arXiv:2402.07987 [quant-ph].

[83] E. M. Murairi, M. J. Cervia, H. Kumar, P. F. Bedaque, and A. Alexandru, How many quantum gates do gauge theories require? (2022), arXiv:2208.11789 [hep-lat].

[84] E. Zohar, J. I. Cirac, and B. Reznik, Quantum Simulations of Lattice Gauge Theories using Ultracold Atoms in Optical Lattices, Rept. Prog. Phys. **79**, 014401 (2016), arXiv:1503.02312 [quant-ph].

[85] E. Zohar, J. I. Cirac, and B. Reznik, Cold-Atom Quantum Simulator for SU(2) Yang-Mills Lattice Gauge Theory, Phys. Rev. Lett. **110**, 125304 (2013), arXiv:1211.2241 [quant-ph].

[86] E. Zohar, J. I. Cirac, and B. Reznik, Simulating Compact Quantum Electrodynamics with ultracold atoms: Probing confinement and nonperturbative effects, Phys. Rev. Lett. **109**, 125302 (2012), arXiv:1204.6574 [quant-ph].

[87] E. Zohar, J. I. Cirac, and B. Reznik, Quantum simulations of gauge theories with ultracold atoms: local gauge invariance from angular momentum conservation, Phys. Rev. **A88**, 023617 (2013), arXiv:1303.5040 [quant-ph].

[88] J. a. Barata, N. Mueller, A. Tarasov, and R. Venugopalan, Single-particle digitization strategy for quantum computation of a ϕ^4 scalar field theory (2020), arXiv:2012.00020 [hep-th].

[89] E. Zohar and M. Burrello, Formulation of lattice gauge theories for quantum simulations, Phys. Rev. **D91**, 054506 (2015), arXiv:1409.3085 [quant-ph].

[90] M. Kreshchuk, W. M. Kirby, G. Goldstein, H. Beauchemin, and P. J. Love, Quantum Simulation of Quantum Field Theory in the Light-Front Formulation (2020), arXiv:2002.04016 [quant-ph].

[91] M. Kreshchuk, S. Jia, W. M. Kirby, G. Goldstein, J. P. Vary, and P. J. Love, Simulating Hadronic Physics on NISQ devices using Basis Light-Front Quantization (2020), arXiv:2011.13443 [quant-ph].

[92] M. Kreshchuk, S. Jia, W. M. Kirby, G. Goldstein, J. P. Vary, and P. J. Love, Light-Front Field Theory on Current Quantum Computers (2020), arXiv:2009.07885 [quant-ph].

[93] J. Liu and Y. Xin, Quantum simulation of quantum field theories as quantum chemistry (2020), arXiv:2004.13234 [hep-th].

[94] M. Fromm, O. Philipsen, W. Unger, and C. Winterowd, Quantum Gate Sets for Lattice QCD in the strong coupling limit: $N_f = 1$ (2023), arXiv:2308.03196 [hep-lat].

[95] T. Li, Quantum simulations of quantum electrodynamics in Coulomb gauge (2024), arXiv:2406.01204 [hep-lat].

[96] A. Hardy *et al.*, Optimized Quantum Simulation Algorithms for Scalar Quantum Field Theories (2024), arXiv:2407.13819 [quant-ph].

[97] J. a. Barata, K. Ikeda, S. Mukherjee, and J. Raghoonanan, Towards Quantum Computing Timelike Hadronic Vacuum Polarization and Light-by-Light Scattering: Schwinger Model Tests (2024), arXiv:2406.03536 [hep-ph].

[98] E. Gustafson, Y. Meurice, and J. Unmuth-Yockey, Quantum simulation of scattering in the quantum Ising model, Phys. Rev. D **99**, 094503 (2019), arXiv:1901.05944 [hep-lat].

[99] T. D. Cohen, H. Lamm, S. Lawrence, and Y. Yamauchi (NuQS), Quantum algorithms for transport coefficients in gauge theories, Phys. Rev. D **104**, 094514 (2021).

[100] H. Lamm, S. Lawrence, and Y. Yamauchi (NuQS), Parton physics on a quantum computer, Phys. Rev. Res. **2**, 013272 (2020), arXiv:1908.10439 [hep-lat].

[101] E. J. Gustafson, H. Lamm, and J. Unmuth-Yockey, Quantum mean estimation for lattice field theory, Phys. Rev. D **107**, 114511 (2023), arXiv:2303.00094 [hep-lat].

[102] E. Zohar, Quantum simulation of lattice gauge theories in more than one space dimension—requirements, challenges and methods, Phil. Trans. A. Math. Phys. Eng. Sci. **380**, 20210069 (2021), arXiv:2106.04609 [quant-ph].

[103] J. Bender, E. Zohar, A. Farace, and J. I. Cirac, Digital quantum simulation of lattice gauge theories in three spatial dimensions, New J. Phys. **20**, 093001 (2018), arXiv:1804.02082 [quant-ph].

[104] R. C. Farrell, I. A. Chernyshev, S. J. M. Powell, N. A. Zemlevskiy, M. Illa, and M. J. Savage, Preparations for quantum simulations of quantum chromodynamics in 1+1 dimensions. I. Axial gauge, Phys. Rev. D **107**, 054512 (2023), arXiv:2207.01731 [quant-ph].

[105] R. C. Farrell, I. A. Chernyshev, S. J. M. Powell, N. A. Zemlevskiy, M. Illa, and M. J. Savage, Preparations for quantum simulations of quantum chromodynamics in 1+1 dimensions. II. Single-baryon β-decay in real time, Phys. Rev. D **107**, 054513 (2023), arXiv:2209.10781 [quant-ph].

[106] H.-H. Lu *et al.*, Simulations of Subatomic Many-Body Physics on a Quantum Frequency Processor, Phys. Rev. A **100**, 012320 (2019), arXiv:1810.03959 [quant-ph].

[107] D. M. Kurkcuoglu, M. S. Alam, J. A. Job, A. C. Y. Li, A. Macridin, G. N. Perdue, and S. Providence, Quantum simulation of ϕ^4 theories in qudit systems (2022), arXiv:2108.13357 [quant-ph].

[108] E. Zohar, A. Farace, B. Reznik, and J. I. Cirac, Digital lattice gauge theories, Phys. Rev. **A95**, 023604 (2017), arXiv:1607.08121 [quant-ph].

[109] M. Illa and M. J. Savage, Basic elements for simula-

tions of standard-model physics with quantum annealers: Multigrid and clock states, Phys. Rev. A **106**, 052605 (2022), arXiv:2202.12340 [quant-ph].

[110] P. P. Popov, M. Meth, M. Lewenstein, P. Hauke, M. Ringbauer, E. Zohar, and V. Kasper, Variational quantum simulation of U(1) lattice gauge theories with qudit systems, Phys. Rev. Res. **6**, 013202 (2024).

[111] N. Klco and M. J. Savage, Minimally entangled state preparation of localized wave functions on quantum computers, Phys. Rev. A **102**, 012612 (2020), arXiv:1904.10440 [quant-ph].

[112] J. C. Halimeh and P. Hauke, Staircase prethermalization and constrained dynamics in lattice gauge theories (2020), arXiv:2004.07248 [cond-mat.quant-gas].

[113] R. C. Farrell, M. Illa, and M. J. Savage, Steps Toward Quantum Simulations of Hadronization and Energy-Loss in Dense Matter (2024), arXiv:2405.06620 [quant-ph].

[114] E. Gustafson, Projective Cooling for the transverse Ising model, Phys. Rev. D **101**, 071504 (2020), arXiv:2002.06222 [hep-lat].

[115] A. Avkhadiev, P. E. Shanahan, and R. D. Young, Accelerating Lattice Quantum Field Theory Calculations via Interpolator Optimization Using Noisy Intermediate-Scale Quantum Computing, Phys. Rev. Lett. **124**, 080501 (2020).

[116] M. Carena, H. Lamm, Y.-Y. Li, and W. Liu, Lattice renormalization of quantum simulations, Phys. Rev. D **104**, 094519 (2021), arXiv:2107.01166 [hep-lat].

[117] M. Carena, E. J. Gustafson, H. Lamm, Y.-Y. Li, and W. Liu, Gauge theory couplings on anisotropic lattices, Phys. Rev. D **106**, 114504 (2022), arXiv:2208.10417 [hep-lat].

[118] P. Emonts and E. Zohar, Gauss law, Minimal Coupling and Fermionic PEPS for Lattice Gauge Theories, in *Tensor Network and entanglement* (2018) arXiv:1807.01294 [quant-ph].

[119] A. Avkhadiev, P. E. Shanahan, and R. D. Young, Strategies for quantum-optimized construction of interpolating operators in classical simulations of lattice quantum field theories, Phys. Rev. D **107**, 054507 (2023), arXiv:2209.01209 [hep-lat].

[120] G. T. Fleming, P. Shyamsundar, and J. Unmuth-Yockey, Fermion determinants on a quantum computer (2024), arXiv:2407.13080 [hep-lat].

[121] A. Crippa, S. Romiti, L. Funcke, K. Jansen, S. Kühn, P. Stornati, and C. Urbach, Towards determining the (2+1)-dimensional Quantum Electrodynamics running coupling with Monte Carlo and quantum computing methods (2024), arXiv:2404.17545 [hep-lat].

[122] Y. Guo, T. Angelides, K. Jansen, and S. Kühn, Concurrent VQE for Simulating Excited States of the Schwinger Model (2024), arXiv:2407.15629 [quant-ph].

[123] H. Lamm, S. Lawrence, and Y. Yamauchi (NuQS), Suppressing Coherent Gauge Drift in Quantum Simulations (2020), arXiv:2005.12688 [quant-ph].

[124] M. Carena, H. Lamm, Y.-Y. Li, and W. Liu, Quantum error thresholds for gauge-redundant digitizations of lattice field theories (2024), arXiv:2402.16780 [hep-lat].

[125] J. C. Halimeh, R. Ott, I. P. McCulloch, B. Yang, and P. Hauke, Robustness of gauge-invariant dynamics against defects in ultracold-atom gauge theories, Phys. Rev. Res. **2**, 033361 (2020), arXiv:2005.10249 [cond-mat.quant-gas].

[126] J. C. Halimeh, H. Lang, and P. Hauke, Gauge protection in non-Abelian lattice gauge theories (2021), arXiv:2106.09032 [cond-mat.quant-gas].

[127] M. C. Tran, Y. Su, D. Carney, and J. M. Taylor, Faster Digital Quantum Simulation by Symmetry Protection (2020), arXiv:2006.16248 [quant-ph].

[128] J. C. Halimeh and P. Hauke, Reliability of lattice gauge theories (2019), arXiv:2001.00024 [cond-mat.quant-gas].

[129] J. C. Halimeh, V. Kasper, and P. Hauke, Fate of Lattice Gauge Theories Under Decoherence (2020), arXiv:2009.07848 [cond-mat.quant-gas].

[130] J. C. Halimeh, H. Lang, J. Mildenberger, Z. Jiang, and P. Hauke, Gauge-Symmetry Protection Using Single-Body Terms, PRX Quantum **2**, 040311 (2021), arXiv:2007.00668 [quant-ph].

[131] V. Kasper, T. V. Zache, F. Jendrzejewski, M. Lewenstein, and E. Zohar, Non-Abelian gauge invariance from dynamical decoupling, Phys. Rev. D **107**, 014506 (2023), arXiv:2012.08620 [quant-ph].

[132] M. Carena, H. Lamm, Y.-Y. Li, and W. Liu, Improved Hamiltonians for Quantum Simulations of Gauge Theories, Phys. Rev. Lett. **129**, 051601 (2022).

[133] A. N. Ciavarella and C. W. Bauer, Quantum Simulation of SU(3) Lattice Yang Mills Theory at Leading Order in Large N (2024), arXiv:2402.10265 [hep-ph].

[134] E. J. Gustafson, Stout Smearing on a Quantum Computer (2022), arXiv:2211.05607 [hep-lat].

[135] E. Murairi, S. Alam, S. Hadfield, H. Lamm, and E. J. Gustafson, Subgroup adapted quantum Fourier transforms for a set of nonabelian finite groups, in preparation (2024).

[136] E. Zohar and J. I. Cirac, Removing Staggered Fermionic Matter in $U(N)$ and $SU(N)$ Lattice Gauge Theories, Phys. Rev. D **99**, 114511 (2019), arXiv:1905.00652 [quant-ph].

[137] E. Zohar and J. I. Cirac, Eliminating fermionic matter fields in lattice gauge theories, Phys. Rev. B **98**, 075119 (2018), arXiv:1805.05347 [quant-ph].

[138] E. Gustafson, Prospects for Simulating a Qudit Based Model of (1+1)d Scalar QED, Phys. Rev. D **103**, 114505 (2021), arXiv:2104.10136 [quant-ph].

[139] E. Gustafson, Noise Improvements in Quantum Simulations of sQED using Qutrits (2022), arXiv:2201.04546 [quant-ph].

[140] M. Illa, C. E. P. Robin, and M. J. Savage, Qu8its for quantum simulations of lattice quantum chromodynamics (2024), arXiv:2403.14537 [quant-ph].

[141] E. Gustafson *et al.*, Large scale multi-node simulations of $\mathbb{Z}_2$ gauge theory quantum circuits using Google Cloud Platform, in *IEEE/ACM Second International Workshop on Quantum Computing Software* (2021) arXiv:2110.07482 [quant-ph].

[142] E. Gustafson, P. Dreher, Z. Hang, and Y. Meurice, Benchmarking quantum computers for real-time evolution of a (1+1) field theory with error mitigation, Quantum Sci. Technol. **6**, 045020 (2021), arXiv:1910.09478 [hep-lat].

[143] B. Chakraborty, M. Honda, T. Izubuchi, Y. Kikuchi, and A. Tomiya, Classically emulated digital quantum simulation of the schwinger model with a topological term via adiabatic state preparation, Phys. Rev. D **105**, 094503 (2022).

[144] Z. Davoudi, N. Mueller, and C. Powers, Towards Quantum Computing Phase Diagrams of Gauge Theories

with Thermal Pure Quantum States, Phys. Rev. Lett. **131**, 081901 (2023).

[145] M. Honda, E. Itou, Y. Kikuchi, L. Nagano, and T. Okuda, Classically emulated digital quantum simulation for screening and confinement in the schwinger model with a topological term, Phys. Rev. D **105**, 014504 (2022).

[146] N. Mueller, J. A. Carolan, A. Connelly, Z. Davoudi, E. F. Dumitrescu, and K. Yeter-Aydeniz, Quantum Computation of Dynamical Quantum Phase Transitions and Entanglement Tomography in a Lattice Gauge Theory, PRX Quantum **4**, 030323 (2023), arXiv:2210.03089 [quant-ph].

[147] Z. Davoudi, C.-C. Hsieh, and S. V. Kadam, Scattering wave packets of hadrons in gauge theories: Preparation on a quantum computer (2024), arXiv:2402.00840 [quant-ph].

[148] W. A. de Jong, K. Lee, J. Mulligan, M. Płoskoń, F. Ringer, and X. Yao, Quantum simulation of nonequilibrium dynamics and thermalization in the schwinger model, Phys. Rev. D **106**, 054508 (2022).

[149] X.-D. Xie, X. Guo, H. Xing, Z.-Y. Xue, D.-B. Zhang, and S.-L. Zhu (QuNu Collaboration), Variational thermal quantum simulation of the lattice schwinger model, Phys. Rev. D **106**, 054509 (2022).

[150] A. F. Shaw, P. Lougovski, J. R. Stryker, and N. Wiebe, Quantum Algorithms for Simulating the Lattice Schwinger Model, Quantum **4**, 306 (2020).

[151] A. Florio, D. Frenklakh, K. Ikeda, D. E. Kharzeev, V. Korepin, S. Shi, and K. Yu, Quantum simulation of entanglement and hadronization in jet production: lessons from the massive Schwinger model (2024), arXiv:2404.00087 [hep-ph].

[152] I. Papaefstathiou, J. Knolle, and M. C. Bañuls, Real-time scattering in the lattice Schwinger model (2024), arXiv:2402.18429 [hep-lat].

[153] For faster convergence to the continuum limit, one may replace $m_0 \to m_{lat.} \equiv m_0 - \frac{ag^2}{8}$ in Eq. (1) which greatly reduces errors from discretization [**?**]. In this work we ignore this correction, simply to provide a demonstration of the efficacy of $(SC)^2$-ADAPT-VQE.

[154] C. Feniou, M. Hassan, D. Traoré, E. Giner, Y. Maday, and J.-P. Piquemal, Overlap-adapt-vqe: practical quantum chemistry on quantum computers via overlap-guided compact ansätze, Communications Physics **6**, 10.1038/s42005-023-01312-y (2023).

[155] H. L. Tang, V. Shkolnikov, G. S. Barron, H. R. Grimsley, N. J. Mayhall, E. Barnes, and S. E. Economou, Qubit-adapt-vqe: An adaptive algorithm for constructing hardware-efficient ansätze on a quantum processor, PRX Quantum **2**, 020310 (2021).

[156] Y. S. Yordanov, V. Armaos, C. H. W. Barnes, and D. R. M. Arvidsson-Shukur, Qubit-excitation-based adaptive variational quantum eigensolver, Communications Physics **4**, 1 (2021).

[157] V. O. Shkolnikov, N. J. Mayhall, S. E. Economou, and E. Barnes, Avoiding symmetry roadblocks and minimizing the measurement overhead of adaptive variational quantum eigensolvers, Quantum **7**, 1040 (2023).

[158] M. Ramôa, P. G. Anastasiou, L. P. Santos, N. J. Mayhall, E. Barnes, and S. E. Economou, Reducing the resources required by adapt-vqe using coupled exchange operators and improved subroutines (2024), arXiv:2407.08696 [quant-ph].

[159] J. Lee, W. J. Huggins, M. Head-Gordon, and K. B. Whaley, Generalized unitary coupled cluster wave functions for quantum computation, Journal of chemical theory and computation **15**, 311 (2018).

[160] N. K. Nielsen and B. Schroer, Topological Fluctuations and Breaking of Chiral Symmetry in Gauge Theories Involving Massless Fermions, Nucl. Phys. B **120**, 62 (1977).

[161] G. 't Hooft, A Two-Dimensional Model for Mesons, Nucl. Phys. B **75**, 461 (1974).

[162] J. Glimm and A. M. Jaffe, A LAMBDA PHI**4 QUANTUM FIELD THEORY WITHOUT CUTOFFS. 1, Phys. Rev. **176**, 1945 (1968).

[163] V. A. Rubakov and A. N. Tavkhelidze, Stable Anomalous States of Superdense Matter in Gauge Theories, Phys. Lett. B **165**, 109 (1985).

[164] A. Florio, A. Weichselbaum, S. Valgushev, and R. D. Pisarski, Mass gaps of a $\mathbb{Z}_3$ gauge theory with three fermion flavors in 1 + 1 dimensions (2023), arXiv:2310.18312 [hep-th].